

## THE FORMATION OF COSMIC FULLERENES FROM AROPHATIC CLUSTERS

ELISABETTA R. MICELOTTA<sup>1</sup>

Department of Physics and Astronomy, University of Western Ontario,  
London, Ontario N6A 3K7, Canada

ANTHONY P. JONES<sup>2</sup>

Institut d'Astrophysique Spatiale, CNRS/Université Paris Sud, 91405 Orsay, France

JAN CAMI<sup>1, 3</sup> AND ELS PEETERS<sup>1, 3</sup>

Department of Physics and Astronomy, University of Western Ontario,  
London, Ontario N6A 3K7, Canada

JERONIMO BERNARD-SALAS<sup>2</sup>

Institut d'Astrophysique Spatiale, CNRS/Université Paris Sud, 91405 Orsay, France

AND

GIOVANNI FANCHINI<sup>1</sup>

Department of Physics and Astronomy, University of Western Ontario,  
London, Ontario N6A 3K7, Canada

*Draft version August 3, 2018*

### ABSTRACT

Fullerenes have recently been identified in space and they may play a significant role in the gas and dust budget of various astrophysical objects including planetary nebulae (PNe), reflection nebulae (RNe) and HII regions. The tenuous nature of the gas in these environments precludes the formation of fullerene materials following known vaporization or combustion synthesis routes even on astronomical timescales. We have studied the processing of hydrogenated amorphous carbon (a-C:H or HAC) nanoparticles and their specific derivative structures, which we name “arophatics”, in the circumstellar environments of young, carbon-rich PNe. We find that UV-irradiation of such particles can result in the formation of fullerenes, consistent with the known physical conditions in PNe and with available timescales.

*Subject headings:* circumstellar matter – infrared: general – ISM: molecules – planetary nebulae: general – stars: AGB and post-AGB

### 1. INTRODUCTION

The gas and dust that is ejected by dying stars and from which new stars will form, is constantly being processed chemically as well as physically (*e.g.*, Tielens 2005). A particularly rich and diverse route is followed by carbon. In the cool surroundings of carbon stars – evolved stars that have dredged up large amounts of carbon to the stellar surface – more than 60 individual molecular species have been identified, including benzene, polyynes and cyanopolyynes (Kwok 2009; Cernicharo et al. 2001; Pardo et al. 2007). In addition, the spectra reveal diverse dusty materials such as hydrogenated amorphous carbon (HAC or a-C:H) and silicon carbide (SiC). As the mass-loss process strips the outer layers of the star, a hot ( $T \geq 30,000$  K) central white dwarf becomes exposed, whose strong UV irradiation further processes the ejecta and makes them visible as a planetary nebula (PN). A key component of the carbon dust inventory in PNe are polycyclic aromatic hydrocarbons (PAHs) and PAH-like species, a class of large

and hardy carbonaceous species whose formation mechanisms are unclear (Cherchneff et al. 2000). Although not a single PAH member has been identified in space, their characteristic spectral features at infrared wavelengths are observed throughout the Universe, from which it is inferred that they reside ubiquitously in space and could lock up as much as 15% of the cosmic carbon (*e.g.*, Tielens 2005).

Two other large aromatic species have been recently identified in space: C<sub>60</sub> and C<sub>70</sub>. These are the best-known members of the family of fullerenes, a class of molecules made of hexagonal and pentagonal aromatic carbon rings, fused in the shape of a hollow sphere or ellipsoid. The most abundant of these molecules, the Buckminsterfullerene C<sub>60</sub>, has the structure of an old-fashioned black and white soccer ball. The near-spherical carbon configuration of these two molecules, which have a closed surface, a closed-shell electron distribution and an almost unstrained network, results in a very high stability against dissociation and prolonged exposure to high temperature. Fullerenes, in particular C<sub>60</sub>, have peculiar and appealing photochemical, electrochemical and physical properties, which can be exploited in various fields, from nanotechnology to medicine, to space

email: emicelot@uwo.ca

<sup>3</sup> SETI Institute, 189 Bernardo Avenue, Suite 100, Mountain View, CA 94043, USA

science.

$C_{60}$  and  $C_{70}$  were discovered during laser ablation experiments on graphite targets, aiming to study long carbon chains in interstellar clouds (Kroto et al. 1985). Because of their remarkable stability, fullerenes appeared particularly suited to survive the harsh conditions of the interstellar medium. Their unique properties indicate that they may play an important role in organic astrochemistry and astrobiology. Cosmic fullerenes remained elusive until the recent discovery of  $C_{60}$  and  $C_{70}$  in the planetary nebula Tc 1 by Cami et al. (2010). Fullerenes have since been confirmed in many more evolved star environments (García-Hernández et al. 2010, 2011b; Zhang & Kwok 2011; Clayton et al. 2011; Gielen et al. 2011; Roberts et al. 2012; Evans et al. 2012), as well as in young stellar objects (Roberts et al. 2012), reflection nebulae (RNe) (Sellgren et al. 2010; Peeters et al. 2012) and photodissociation regions (Rubin et al. 2011).

Fullerenes can be efficiently synthesized in the laboratory by the vaporization of carbon rods in an electric arc (Krätschmer et al. 1990a,b) and from hydrocarbon combustion under optimised conditions (Howard et al. 1991; Nano-C 2004). However, the formation routes of fullerenes in space are still unknown. We review the currently known formation mechanisms of fullerenes in the laboratory (§ 2), showing why these methods would not work in space (§ 3). We propose an alternative pathway, consistent with astrophysical conditions, based on the photo-processing of a family of carbonaceous species which we name “arophatics” (§ 4). We discuss the observations of fullerenes in PNe (§ 5) and finally we summarize our conclusions (§ 6).

## 2. FULLERENE FORMATION ON EARTH

### 2.1. *The discovery of fullerene*

The original discovery of  $C_{60}$  and  $C_{70}$  dates back to 1985 with the experiment of Kroto et al. (1985). In this experiment, carbon species were vaporized from a graphite target into a He flow with tunable pressure/density. The vaporization was done by a pulsed laser, the resulting carbon clusters were expanded in a supersonic molecular beam, photoionized and their masses measured by a time-of-flight mass spectrometer. Vaporization at low He pressure (less than 10 torr) leads to a broad distribution of clusters, with 38 to 120 carbon atoms (always even numbers), with  $C_{60}$  and  $C_{70}$  present but not the dominant species. At a pressure of 760 torr the  $C_{60}$  and  $C_{70}$  peaks clearly dominated. When the expansion of the He+carbon cluster mixture was delayed, the resulting mass distribution was completely dominated by  $C_{60}$  - 50% of total large cluster abundance, and  $C_{70}$ , with 5 % of total large cluster abundance. These distributions have been interpreted as due to the increasing number of He-cluster and cluster-cluster collisions, resulting in the “survival of the fittest”, i.e. the more stable clusters. The famous icosahedral soccer ball structure was proposed for the first time for  $C_{60}$ , and later confirmed by spectroscopic studies (Krätschmer et al. 1990a,b; Taylor et al. 1990). However, the elementary reaction mechanisms occurring during the “thermalization” process remained unknown.

### 2.2. *The role of temperature: mutually exclusive formation of PAHs and fullerenes*

Jäger et al. (2009) experimentally studied the gas-phase formation of carbonaceous compounds. Their first experiment was essentially a replication of the Kroto experiment, i.e. laser vaporization of a graphite target in a quenching atmosphere of He or He/ $H_2$  with pressures between 3.3 and 26.7 mbar. The vibrational temperature of the laser-induced plasma was estimated to be between 4000 and 6000 K for the laser power densities used. In a second set of experiments, the laser-induced pyrolysis of  $C_2H_2$  and  $C_6H_6$  using a pulsed laser with high power densities was studied. The resulting condensation temperatures were above 3500 K, comparable with the vaporization experiment. In a third set of experiments, laser-induced pyrolysis of the same hydrocarbon precursors was carried out, but this time at a much lower temperature (max 1700 K).

The analysis of the condensation products showed a striking effect of the temperature. During the high temperature experiments, only fullerene-like soot and fullerenes were produced. During the low temperature experiments, only soot and PAHs were formed (100 % PAHs at  $\sim 1000$  K). The results clearly tell that the temperature determines which kind of condensates will be formed. Moreover, the two pathways seem to be mutually exclusive, at least under these experimental conditions: fullerenes and PAHs cannot be formed together. It is important to note that high pressure has been used during the experiments to concentrate the condensation within a small volume, i.e. to maintain a high density of the condensing species.

### 2.3. *Molecular dynamics simulations of fullerene formation*

The laboratory experiments described in the previous sections do not tell us how fullerene is formed from graphite and hydrocarbons, but only under which conditions this happens. The elementary reaction mechanisms involved in the formation of fullerenes can be investigated performing quantum chemical molecular dynamics simulations (Zheng et al. 2005; Irle et al. 2006; Zheng et al. 2007). In one set of simulations a hot carbon vapor was reproduced by putting 40 randomly oriented  $C_2$  molecules in a tiny 20 Å cubic box (Zheng et al. 2005; Zheng et al. 2007). The system was let to evolve, and extra  $C_2$  molecules were added at fixed times in order to simulate an open environment. During the first stage, the system was kept at a constant temperature of 2000 K and giant carbon cages self-assembled. During the second stage of the simulation the temperature was raised to 3000 K, and the shrinking of these hot giant fullerenes down to  $C_{65}$  was observed (Zheng et al. 2007).

The formation of the giant cages starts with nucleation of polycyclic structures (hexagons and pentagons) from entangled polyynes chains. This is followed by growth of the structure and finally cage closure similar to the self-capping of open-ended single-walled nanotubes. Because of the rapid gain of energy due to cage closure, the giant fullerenic cages are produced in a vibrationally highly excited state. The excess energy has to be dissipated, either by unimolecular dissociation or collision with other carbon clusters or carrier gas atoms. The simulations

show that the newly produced giant fullerenes inevitably shrink to smaller sizes. All the road maps to fullerene formation proposed by previous models were associated with intermediate structures that are in thermodynamic equilibrium, while a hot carbon vapor is indeed a system far from thermodynamic equilibrium. In the model developed by Irlé, Morokuma and collaborators, for the first time the dynamic self-assembly of fullerene molecules occurs as an irreversible process emerging naturally under the nonequilibrium conditions typical of a hot carbon vapor.

#### 2.4. Direct formation of fullerenes from graphene

The experimental results of Ugarte (1992) have presented evidence of the spontaneous tendency of electron-irradiated graphite to include pentagons in its hexagonal network, hence form curved structures. This has been further confirmed by Chuvilin et al. (2010), who have shown that fullerenes can form directly from graphene in a similar fashion. In the experiment of Chuvilin and co-workers, a sheet of graphene was exposed to a beam of energetic 80 keV electrons. The energy transferred to the graphene results in the loss of carbon atoms from the edges of the sheet. If the size of the graphene flake is not too big (less than a few hundreds of carbon atoms), the loss of carbon atoms at the edge will lead to the formation of pentagons, which triggers the curving of graphene into a bowl-shaped structure. Further carbon removal from the edges using the electron beam will reduce the size of the curved structure until it is sufficiently small to zip up its open edges and isomerize into a closed fullerene structure.

#### 2.5. Formation of fullerenes via closed network growth

Dunk et al. (2012) claim having identified the fundamental processes leading to the formation of fullerenes in a recent experimental work, based on laser vaporization of pure  $C_{60}$  in the presence of carbon vapor. According to this study, fullerenes would self-assemble bottom-up through a closed network growth (CNG) mechanism based on the ingestion of atomic carbon and  $C_2$  clusters. It should be noted that the work from Dunk et al. (2012) provides experimental evidence of the growth of larger fullerenes from pre-existing  $C_{60}$  only. Because the experiments show that the CNG of larger fullerenes does not result in the production of  $C_{60}$ , it is deduced that  $C_{60}$  formation must be a result of CNG from smaller fullerenes. However, the initial formation mechanism of such smaller fullerenes is still under debate.

### 3. FULLERENE FORMATION IN SPACE: WHY TERRESTRIAL METHODS DO NOT WORK

Although all the chemical ingredients and the required temperatures for graphite vaporization and hydrocarbon combustion can be found in astrophysical environments, the densities are far too low to proceed to fullerene formation on reasonable timescales. In space, the most favourable conditions for fullerene formation via vaporization/combustion are found in a post-shock gas. In such environments the fullerene building blocks, i.e.  $C_2$  groups and polycyclic species coming from the fragmentation of PAHs (Micelotta et al. 2010a,b), ought to exist in the required vibrationally excited states. However,

the post-shock carbon densities are low and represent a serious obstacle to fullerene formation. We have derived the scaling rule (Eq. 1) relating the time  $\tilde{\tau}$ , required for fullerene condensation, with the initial density  $n$  of the carbon gas. The details of the calculation are reported in the Appendix. This scaling rule has then been used to estimate the time necessary for the coagulation of fullerenes from a carbon gas with interstellar densities ( $n \sim 10^{-4}$  carbon  $\text{cm}^{-3}$ ). The scaling rule is:

$$\frac{\tilde{\tau}_2}{\tilde{\tau}_1} = \frac{n_1^2}{n_2^2} \Rightarrow \tilde{\tau}_2 = \frac{\tilde{\tau}_1 n_1^2}{n_2^2}, \quad (1)$$

where  $\tilde{\tau}_1$  and  $\tilde{\tau}_2$  are the condensation timescales corresponding to densities  $n_1$  and  $n_2$  respectively. Knowing the density and timescale in simulations,  $n_1$  and  $\tilde{\tau}_1$ , and the density of the interstellar gas,  $n_2$ , we can then calculate the fullerene condensation time in space,  $\tilde{\tau}_2$ . We adopt  $n_1 = 10^{22}$  carbon  $\text{cm}^{-3}$  and  $\tilde{\tau}_1 = 50$  ps (Zheng et al. 2005). The hydrogen density of the post-shock gas is  $\sim 1$   $\text{cm}^{-3}$ , but carbon is  $10^{-4}$  less abundant, so  $n_2 = 10^{-4}$  carbon  $\text{cm}^{-3}$ . From Eq. 1 we obtain  $\tilde{\tau}_2 = 1.6 \times 10^{34}$  yr, which is longer than the age of the Universe. We also estimate the carbon density  $n_2$  required to form fullerenes in a shocked gas before the temperature drops below 1000 K. At this temperature the condensation of fullerenes cannot occur. For a typical interstellar shock with a velocity of 125  $\text{km s}^{-1}$  the cooling time (after which the temperature of the post-shock gas drops below 1000 K) is about  $2 \times 10^5$  yr. Under these conditions, the required carbon atom density for the condensation of fullerenes is  $n_2 = 3 \times 10^{10}$  carbon  $\text{cm}^{-3}$ , and in space such densities do not exist outside of stellar atmospheres.

Berné & Tielens (2012) propose a scheme for the direct formation of  $C_{60}$  from PAHs in the reflection nebula NGC 7023 based on graphene dissociation experiments from Chuvilin et al. (2010). In NGC 7023 fullerenes and PAHs appear to coexist in the same location close to the central star, while only PAHs are detected further away from the star. According to Berné & Tielens (2012), a similar phenomenon to the one described by Chuvilin et al. (2010) occurs in NGC 7023, but induced by photo processing instead of electron bombardment. The absorption of UV photons from the central star first completely dehydrogenates the PAHs (Tielens 2005), producing graphene flakes. Further photon absorption induces the loss of carbons from the edges of the graphene sheet. This, according to Chuvilin et al. (2010), gives rise to pentagonal defects which will induce the curvature of the sheet and the subsequent closure of the cage to form a  $C_{60}$  molecule.

There are some issues related to the applicability of the results from such experiments to interstellar conditions. First of all, it is not possible in space to tune the number of carbons removed from the graphene flake in order to get the right size required for cage closure. The number of ejected carbons depends on the rather slow photodissociation process, which is governed by the dissociation parameter  $E_0$ . This parameter describes the dissociation rate of a highly excited PAH molecule using an Arrhenius law (Tielens 2005), and to a first approximation can be seen as the energy that needs to be concentrated over a bond in order to break it and release a fragment.

The dissociation probability (and hence the dissociation rate) decreases for increasing  $E_0$  because more energy is required in the bond that has to be broken. The value of  $E_0$  has been derived from experimental data only for very small PAHs (up to 24 C-atoms) with a very open carbon skeleton. The extrapolation of such results to larger ( $\sim 50$  C-atoms) and compact astrophysically relevant PAHs dissociating under interstellar conditions is very uncertain, leading to values of  $E_0$  ranging from 3.65 to 5.6 eV (Micelotta et al. 2010b). This corresponds to values for the dissociation probability going from 0.5 to  $3 \times 10^{-12}$  respectively. To form fullerenes during the lifetime of NGC 7023, the mechanism proposed by Berné & Tielens (2012) needs a specific tuning of the parameters involved. Because the size of PAHs cannot be controlled as during experiments, the number of carbons in the precursor molecule is severely constrained to about 70 atoms, very close to the 60 carbons required to form  $C_{60}$ . More importantly, the most favourable conditions for dissociation are chosen, i.e., the lowest value for the dissociation parameter,  $E_0 = 3.65$  eV. However, this choice does not appear physically motivated. Indeed, if another legitimate value is adopted for the dissociation parameter, e.g.,  $E_0 = 4.6$  eV (the value falling in the middle of the range determined for  $E_0$  – see Micelotta et al. 2010b), the decrease of the dissociation rate is such that the fragmentation process is far too slow and the conclusion suggested in Berné & Tielens (2012) no longer holds: PAHs with 70 carbon atoms require longer than the lifetime of NGC 7023 to fragment, therefore they cannot be the precursors of the  $C_{60}$  observed at the present epoch.

Thus, none of these mechanisms are feasible in the astrophysical settings where fullerenes have been detected, and hence, alternative routes are needed.

#### 4. OUR PROPOSED FORMATION MECHANISM: FROM A-C:H TO FULLERENE THROUGH AROPHATIC CLUSTERS

Trace amounts of fullerenes have been identified among the dissociation products of UV-irradiated HACs (Scott et al. 1997; Gadallah et al. 2011). Together with fullerene emission, the three PNe Tc 1, SMP LMC 56 and SMP SMC 16 show broad emission plateaus between 6 – 9  $\mu\text{m}$  and between 10 – 13  $\mu\text{m}$ , compatible with emission from H-rich amorphous carbon nanoparticles (Bernard-Salas et al. 2012). This suggests that a viable formation route in space could exist that starts from HAC processing (e.g., García-Hernández et al. 2010, 2011a).

In this study we focus on the formation of fullerenes in the circumstellar environments of proto-planetary nebulae (PPNe) and PNe. HACs are an abundant carbonaceous dust component in both these types of objects (Grishko et al. 2001; Goto et al. 2003). In addition, one of the main characteristics of PNe is their strong radiation field, which will process the HACs.

##### 4.1. Arophatic clusters

In their experiments, Smith (1984) and Scott & Duley (1996) showed that HAC/a-C:H decomposition leads to a low density material ( $\rho \lesssim 1.5 \text{ g cm}^{-3}$ ). In particular, Scott & Duley (1996) and Scott et al. (1997) showed that the decomposition end-product is an aerogel-like material consisting of weakly-connected aromatic “proto-graphitic” or PAH-like clusters in a “friable network”.

The dehydrogenation of small carbonaceous particles, containing less than a few hundred C atoms, will likely lead to structures that resemble the particles seen by Scott et al. (1997) in their experiments and/or the locally aromatic polycyclic hydrocarbons (LAPHs) proposed by Petrie et al. (2003). The particles in the Scott et al. (1997) experiments are found to be small alkanes, unsaturated carbon-chain radicals and small dehydrogenated PAH-like species. After the release of these lighter molecules Scott et al. (1997) observed a strong mass peak near 500 amu ( $\simeq 40$  C atom, proto-graphitic, aromatic clusters) having IR spectra similar to that of HAC/a-C(:H) with absorption and emission features at 3.3, 3.4 and 6.2  $\mu\text{m}$ . The results of these experiments and recent modelling (Jones 2012c) therefore imply an intimate mix of aromatic clusters and aliphatic groups in small carbonaceous species. We note that the LAPH structures studied by Petrie et al. (2003) have compositions in the range  $C_{19}H_{22}$  to  $C_{36}H_{32}$  and contain aromatic domains with only a few rings per domain, which are linked by bridging aliphatic ring systems, and should have IR spectral properties similar to HAC/a-C(:H) materials (e.g., Jones 2012a,b,c).

The conditions required for HAC dehydrogenation are common in space, we can thus expect the formation of LAPH-like species where the aromatic components are bridged by olefinic carbon-containing rings and chains. The key component in these structures is the presence of the aliphatic bridging groups linking the aromatic clusters, in what we here call “arophatic” structures. Such structures, analogous to an aliphatic periphery on PAH molecules (e.g., Rauls & Hornekær 2008), could provide sites for molecular hydrogen formation in PDRs (Jones 2012b). Size-dependent  $\pi - \pi^*$  band considerations indicate that the intrinsic aromatic clusters are indeed most likely to consist of ‘isolated’ two- and three-ring systems in such small hydrocarbon particles (Jones 2012c). The non-aromatic carbon atoms are in the form of “more flexible” short olefinic and/or aliphatic bridging structures such as  $-\text{CH}=\text{CH}-$  and  $-\text{CH}_2-\text{CH}_2-$ . This generic type of structure was also proposed by Grishko & Duley (2000), who suggested that aliphatic cyclo-hydrocarbons are the precursors to aromatic cluster formation in HAC materials. This kind of configuration, with aliphatic chains attached to aromatic sites, is also found in Aromatic-Aliphatic Linked Hydrocarbon (AALH) structures, which appear to have an important role in the nucleation of nanoparticles in soot formation in flames (Chung & Violi 2011). It should be noted that AALHs are small and relatively simple molecules, such as 1,2-di(naphthalen-2-yl)ethane (DNE), while our proposed “arophatic” clusters are bigger and more complex structures.

The aliphatic bridging structures must be quasi-orthogonal to the aromatic species that they bridge and will be unable to transform into aromatic structures without compromising (i.e., destroying) the entire structure. These active sites could, likely, interchange between  $sp^2$  olefinic and radical  $sp^3$  states with dangling bonds, in a kind of isomerisation “flipping” process, which could play a key role in cage closure and fullerene formation in the solid state.

The work of Ferrari & Robertson (2004) indicates that small clusters within a-C(:H) materials are chain-like,

while the larger clusters are three-dimensional, cage-like,  $sp^2$  structures and as Chuvilin et al. (2010) show these cage-like structures have a natural tendency to close-up and form fullerene-like and fullerene structures.

The ‘‘aromatic’’ clusters are structures evolving from larger, amorphous hydrocarbon particles and, from a topological point of view, they will inevitably end up with a tube-like, cup-like or cage-like appearance (*e.g.*, see the two right hand species in Fig. 1 of Petrie et al. 2003). Such structures are ‘‘curled-up’’ or ‘‘folded-over’’, defected graphite (DG) or graphene sheets (Jones 2012a), and we can therefore represent them by their ‘‘flattened-out’’ equivalents as per Fig. 12 in Jones (2012a) but with aromatic domains reduced in size to only a few rings per aromatic cluster (Fig. 1).

The aromatisation of the aliphatic bridges to form pentagons can provide a viable route to fullerene formation in the solid phase via these ‘‘aromatic’’ species. The key process is the dehydrogenation of the aliphatic and olefinic ‘‘bridges’’ which naturally leads to aromatic pentagon formation, as shown in Fig. 2 for small a-C:H particle fragments. It appears that there is a link between small carbonaceous particle dehydrogenation in intense UV radiation fields and the formation of fullerenes, which could explain the observation of fullerenes in circumstellar regions associated with small hydrocarbon grains (*e.g.*, Cami et al. 2010; Garcıa-Hernandez et al. 2010, 2011b; Cami et al. 2011; Bernard-Salas et al. 2012).

#### 4.2. Fullerene formation in space

The mechanism that we propose for fullerene formation in space is the following. The starting point is large, nm-sized, H-rich a-C:H particles containing more than a hundred carbon atoms. UV photolysis by photons with energy above 10 eV dehydrogenates these grains (Jones 2012b) and leads to further changes in the molecular structure – a process that we call **STIR** (**Structural Transformations in Intense Radiation** fields). STIR processing requires constant heating (by photon absorption) to keep the particle in a vibrationally excited state that promotes structural transformations leading to the closing of cage-like structures within the a-C:H nanoparticle. Amorphous carbon nanoparticles can be maintained at thermal-equilibrium temperatures of the order of 100–150 K by photon absorption (for H-rich a-C:H particles with band gaps larger than 1 eV) even at thousands of astronomical units from the central stars of PNe, due to their low emissivity at the long wavelengths where

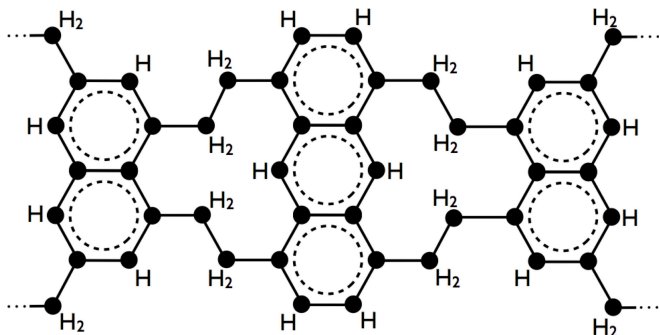


**Figure 1.** An example of an un-wrapped small ‘‘aromatic’’ cluster ( $C_{46}H_{38}$ ). The filled circles represent carbon and the dotted bonds indicate the structure-wrapping connections.

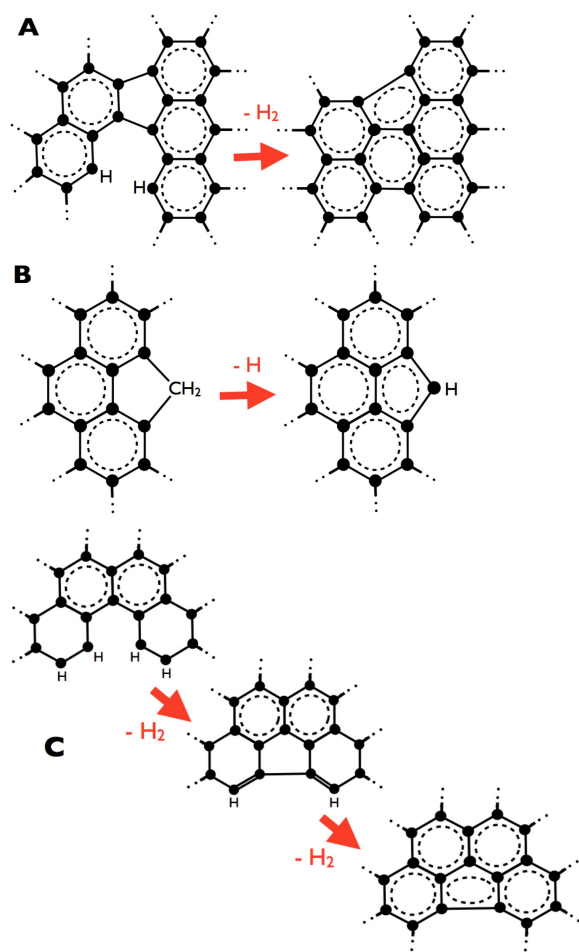


**Figure 2.** A schematic view of three possible routes to aromatic pentagon formation (labeled A, B and C), leading to a loss of planarity, in nm-sized a-C:H particles via aliphatic and olefinic ring system dehydrogenation. The filled circles represent carbon.

they radiate thermally (Bernard-Salas et al. 2012). However, at these same distances, almost completely dehydrogenated nanoparticles have temperatures of only tens of Kelvin, as expected.

In order to form fullerenes, the aromatic clusters resulting from STIR processing must be large, containing more than a hundred carbon atoms, as exemplified in Figs. 3 and 4.

A key step in the route to fullerenes is the formation of 5-membered rings. This can occur via dehydrogenation during the STIR processing of the parent a-C:H or of the emerging aromatic cluster, in a similar fashion as shown in Fig. 2 for small a-C:H particles. Dehydrogenation is a viable way to introduce 5-membered rings, as indicated by Violi (2004). This work shows that structures with a high degree of curvature result from dehydrogenation reactions occurring in aromatic hydrocarbon compounds. These reactions involve the loss of hydrogen with rearrangement of the structure and ring closure which leads to five-membered rings, and hence curvature. UV irradiation of HAC nanoparticles not only causes dehydrogenation (Jones 2012b, and references therein), but also forces the structure to curl up because of the introduction of pentagonal rings. In fact, the UV-induced dehydrogenation *is* the cause of the formation of 5-membered rings.

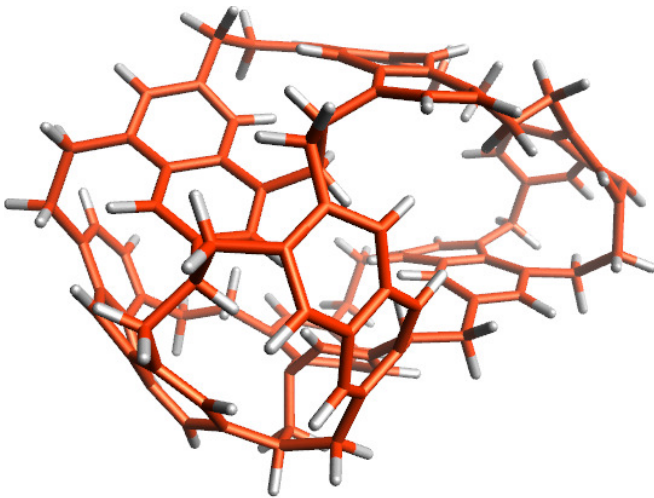


**Figure 3.** The wrapped version of a large and complex “aromatic” cluster ( $C_{104}H_{80}$ ), precursor of cosmic fullerenes. Carbon is represented in dark grey, hydrogen in light gray. The color version of this figure (carbon in red, hydrogen in gray) is available in the electronic edition of the *Astrophysical Journal*.

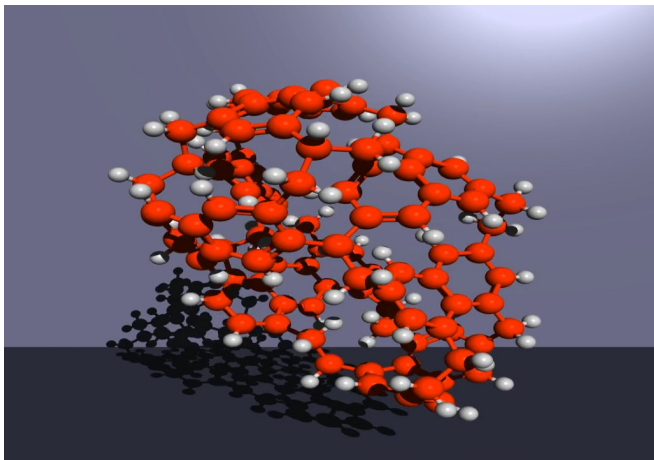


**Figure 4.** A snap-shot from the movie illustrating the 3-D structure of the large and complex “aromatic” cluster  $C_{104}H_{80}$ , precursor of cosmic fullerenes and schematically represented in Fig. 3. Carbon is in dark grey, hydrogen in light gray. The movie, with carbon in red and hydrogen in gray, is available in the electronic edition of the *Astrophysical Journal*.

Thus, in a single step, dehydrogenation fulfills two essential conditions for the formation of fullerene molecules: 1) removing hydrogen atoms and 2) triggering pentagonal ring formation in the evolving structure.

The fullerene precursor is a big and complex aromatic cluster, with the aromatic domains being non-co-planar. The 3-D structure favors the formation of 5-membered aromatic rings, and then curvature, even in such a big structure, via photo-induced dehydrogenation. The particle emerging from the dehydrogenation process is a giant fullerene cage similar to the ones formed in simulations (Irle et al. 2006). The initial, STIR-driven (catastrophic) photolysis and the following cage closure induced by the formation of pentagonal rings will result in a highly excited structure. The cage will release the excess energy via ejection of  $C_2$  molecules, shrinking down to the islands of stability represented by  $C_{60}$  and  $C_{70}$  (Irle et al. 2006). The down-sizing occurs through unimolec-

**Table 1**

Timescale,  $t_s$ , for shrinking of the fullerene cage  $C_{144}$  to  $C_{60}$ .

$T$ (K)	$k_s$ (C/s)	$t_s$ (s)
1000	$1.8 \times 10^9$	$4.7 \times 10^{-8}$
300	$1.1 \times 10^5$	$0.7 \times 10^{-3}$
200	$1.0 \times 10^2$	$8.4 \times 10^{-1}$
100	$1.0 \times 10^{-7}$	$8.4 \times 10^8$

**Note.** —  $T$  is the temperature of the cage and  $k_s$  is the rate for carbon ejection measured in carbon atom lost per second.

ular decomposition of the vibrationally excited cage, resulting in the ejection of carbon molecules. To model the unimolecular dissociation we adopt an Arrhenius law (Tielens 2005), which describes the evolution of the dissociation rate as a function of the temperature of the dissociating species:

$$k_s(T) = k_0 \exp(-E_0/kT) \quad (2)$$

The quantity  $k_s$  is the rate for carbon ejection measured in carbon atom lost per second (C/s),  $T$  the vibrational temperature of the fullerene cage and  $k$  the Boltzmann constant. The unimolecular decomposition is governed by two parameters: the pre-exponential factor  $k_0$  and the dissociation energy  $E_0$ . To estimate the value of these two parameters, we use two sets of simulations which follow the shrinking of giant fullerene cages at two different temperatures, 2000 and 3000 K, and provide the corresponding dissociation rates. The average dissociation rate  $k_s$  is  $1.5 \times 10^{10}$  C/s and  $3 \times 10^{10}$  C/s for  $T = 2000$  K and  $T = 3000$  K respectively (Zheng et al. 2007). We obtain the following values for  $k_0$  and  $E_0$ :

$$\begin{aligned} k_0 &= 1.2 \times 10^{11} \text{ C/s} \\ E_0 &= 0.36 \text{ eV} \end{aligned}$$

The time  $t_s$  required for a big fullerene cage to shrink down to  $C_{60}$  is given by:

$$t_s(T) = N_{ej}/k_s(T) \quad (3)$$

where  $N_{ej}$  is the number of carbons that have to be ejected from the cage and  $k_s$  is the ejection rate from Eq. 2. We consider a fullerene cage containing 144 carbon atoms, i.e. with size comparable to the size of the particles considered in simulations (Zheng et al. 2007), therefore,  $N_{ej} = 84$ . The shrinking timescales for various temperatures of the initial cage are reported in Table 1. This process requires relatively short time scales: to shrink a large (144 carbon atoms) fullerene cage to  $C_{60}$  requires only about 0.8 s at 200 K, and increases to 27 years at 100 K.

To the best of our knowledge, our extrapolation is the first attempt to characterize the shrinking of a giant fullerene cage under interstellar conditions (e.g., very low temperatures with respect to the usual laboratory conditions). The value of 0.36 eV that we have calculated for  $E_0$  should be considered as a lower limit, having been determined under the most favourable conditions for fullerene formation on Earth, as indicated by simulations (nevertheless the optimized conditions for industrial production of fullerene are quite similar). The issue that we are facing here is another example of the well known problem related to the extrapolation to extraterrestrial

conditions of the results from statistical unimolecular dissociation theories (Tielens 2005; Micelotta et al. 2010b). The proper evaluation of  $E_0$  and of the uncertainty associated with it requires the development of a specific model which will be the subject of a following paper. Our present scope is to provide a first indication of the timescales associated with the shrinking process in space. In the case of PAH dissociation under extraterrestrial conditions, the detailed evaluation of the dissociation parameter  $E_0$  resulted in a factor of 10 uncertainty on the calculated fragmentation timescales (Micelotta et al. 2010b). Because of the similarities between large PAHs and fullerenes (Micelotta et al. 2010a,b), we can consider a  $10^2$  uncertainty for the fullerene shrinking timescale as a very conservative assumption. We obtain then a maximum shrinking time of 2670 years at  $T=100$  K (the least favourable condition). This is fully consistent with the age of young PNe where fullerenes have been observed.

$C_{60}$  and  $C_{70}$  are the only, and therefore smallest,  $C_n$  fullerenes with  $n \leq 70$  satisfying the Isolated Pentagon Rule (IPR). This implies (almost) spherical, thermodynamically favored, closed shell structures particularly suited to survive harsh conditions. The shrinking stops at  $C_{60}$  because of the very high Arrhenius dissociation energy  $E_0$  for  $C_2$  elimination to  $C_{58}$ ,  $E_0 \sim 10$  eV (Tomita et al. 2001). The estimated temperatures of a few hundreds of Kelvin for fullerenes detected in planetary nebulae (Cami et al. 2010; Bernard-Salas et al. 2012) are far from the approximately 1000 K required to overcome this decomposition barrier (Leifer et al. 1995).

Our model proposes the formation of a single  $C_{60}$  ( $C_{70}$ ) molecule from a single large aromatic cluster. This implies that the parent a-C:H particles must be nm-sized, and therefore contain a hundred or more carbon atoms, because of the dissociative loss of carbon (and hydrogen) atoms that will occur during structural transformation. Note that the large aromatic clusters can be further fragmented by the same radiation field that caused their formation from the parent a-C:H grain. Most of the formed aromatics will fragment into structures other than fullerenes, resulting in a fullerene formation process that is rather inefficient, consistent with the low fullerene abundance observed in space so far.

## 5. FULLERENE OBSERVATIONS IN PLANETARY NEBULAE

The peculiarities of the PNe where fullerenes have been detected are their intense UV radiation fields, sufficient to sustain photo-chemical processing of HACs, and the ablation of carbonaceous material from the dense circumstellar matter formed during their AGB phase. Thus, in these objects abundant, nm-sized, H-rich, a-C:H dust is being liberated and undergoing catastrophic UV-photolysis, which leads to STIR processing. In Tc 1,  $C_{60}$  and  $C_{70}$  have been detected far from the central star (8000 AU – Bernard-Salas et al. 2012), but even at this distance the UV irradiation is sufficient to keep the particles in a vibrationally excited state ( $T \sim 100$ -130 K) and to trigger and sustain the STIR processing of the a-C:H dust and the shrinking of the resulting giant fullerenic cages down to  $C_{60}$  and  $C_{70}$ .

It appears that the young PNe where fullerenes have been observed are the optimised factories for their formation because their stellar emission peaks in the required

10 eV photon energy regime. In their pre-PNe stages these objects do not have sufficient UV photons to dehydrogenate and heat the dust, and in their later stages the radiation field is so much harder that dissociative losses will destroy the H-rich carbonaceous particles before they can re-structure to form fullerenes.

## 6. CONCLUSIONS

We studied the formation of fullerenes  $C_{60}$  and  $C_{70}$  in planetary nebulae, for which a satisfactory formation path is still missing.

In space, the low density of the gas precludes the formation of fullerene materials following known vaporization or combustion synthesis routes even on astronomical timescales.

The direct formation of  $C_{60}$  through dissociation-induced curvature of dehydrogenated PAHs requires a very specific tuning of the dissociation parameters, and thus appears unlikely.

The scheme for fullerene formation in space that we propose is based on a top-down approach. The top of the tree is represented by large a-C:H/HAC particles, i.e. materials whose presence in space has been firmly established.

UV photolysis promotes structural transformations in the parent a-C:H particle with the formation of what we call “aromatic” clusters: 3-D, hollow structures characterized by the presence of aromatic clusters linked by aliphatic bridging groups.

UV-induced dehydrogenation of the emerging aromatic cluster (or the parent a-C:H) introduces pentagonal rings, and hence curvature, in the evolving structure.

The result is a large, vibrationally-excited fullerenic cage that shrinks down to the stable molecules  $C_{60}$  and  $C_{70}$  through emission of  $C_2$  groups. The very high energy barrier for  $C_2$  ejection from  $C_{60}$  prevents further dissociation.

The young PNe where fullerenes have been observed appear as the optimised factories for the formation of these molecules. In their pre-PNe stages the formation of fullerene-like structure is not favoured because these objects lack sufficient UV photons to dehydrogenate and heat the dust. In their later stages the radiation field is so much harder that it will destroy H-rich carbonaceous particles before they can re-structure to form fullerenes.

We would like to thank G. Lavaux for the realization of the movie and Fig. 3. E.R.M, J.C. and E.P. acknowledge the support from the National Science and Engineering Research Council of Canada (NSERC). J.B-S. wishes to acknowledge the support from a Marie Curie Intra-European Fellowship within the 7th European Community Framework Program under project number 272820. This research has made use of NASA’s Astrophysics Data System.

## REFERENCES

- Bernard-Salas, J., Cami, J., Peeters, E., et al. 2012, ApJ, 757, 41  
 Berné, O., & Tielens, A. G. G. M. 2012, Proceedings of the National Academy of Science, 109, 401  
 Cami, J., Bernard-Salas, J., Peeters, E., & Malek, S. E. 2010, Science, 329, 1180

- Cami, J., Bernard-Salas, J., Peeters, E., & Malek, S. E. 2011, in IAU Symposium, Vol. 280, IAU Symposium, 216–227
- Cernicharo, J., Heras, A. M., Tielens, A. G. G. M., et al. 2001, *ApJ*, 546, L123
- Cherchneff, I., Le Teuff, Y. H., Williams, P. M., & Tielens, A. G. G. M. 2000, *A&A*, 357, 572
- Chung, S.-H., & Violi, A. 2011, *Proc. Combust. Inst.*, 33, 693
- Chuvilin, A., Kaiser, U., Bichoutskaia, E., Besley, N. A., & Khlobystov, A. N. 2010, *Nature Chemistry*, 2, 450
- Clayton, G. C., De Marco, O., Whitney, B. A., et al. 2011, *AJ*, 142, 54
- Dunk, P. W., Kaiser, N. K., Hendrickson, C. L., et al. 2012, *Nat. Commun.*, 3, 855
- Evans, A., van Loon, J. T., Woodward, C. E., et al. 2012, *MNRAS*, 421, L92
- Ferrari, A. C., & Robertson, J. 2004, *Phil. Trans. R. Soc. Lond. A*, 362, 2477
- Gadallah, K. A. K., Mutschke, H., & Jäger, C. 2011, *A&A*, 528, A56
- García-Hernández, D. A., Kameswara Rao, N., & Lambert, D. L. 2011a, *ApJ*, 729, 126
- García-Hernández, D. A., Manchado, A., García-Lario, P., et al. 2010, *ApJ*, 724, L39
- García-Hernández, D. A., Iglesias-Groth, S., Acosta-Pulido, J. A., et al. 2011b, *ApJ*, 737, L30
- Gielen, C., Cami, J., Bouwman, J., Peeters, E., & Min, M. 2011, *A&A*, 536, A54
- Goto, M., Gaessler, W., Hayano, Y., et al. 2003, *ApJ*, 589, 419
- Grishko, V. I., & Duley, W. W. 2000, *ApJ*, 543, L85
- Grishko, V. I., Tereshchuk, K., Duley, W. W., & Bernath, P. 2001, *ApJ*, 558, L129
- Howard, J. B., McKinnon, J. T., Makarovskiy, Y., Lafleur, A. L., & Johnson, M. E. 1991, *Nature*, 352, 139
- Irle, S., Zheng, G., Wang, Z., & Morokuma, K. 2006, *The Journal of Physical Chemistry B*, 110, 14531, PMID: 16869552
- Jäger, C., Huisken, F., Mutschke, H., Jansa, I. L., & Henning, T. 2009, *ApJ*, 696, 706
- Jones, A. P. 2012a, *A&A*, 540, A1+
- 2012b, *A&A*, 540, A2+
- 2012c, *A&A*, 542, A98+
- Krätschmer, W., Fostiropoulos, K., & Huffman, D. R. 1990a, *Chem. Phys. Lett.*, 170, 167
- Krätschmer, W., Lamb, L. D., Fostiropoulos, K., & Huffman, D. R. 1990b, *Nature*, 347, 354
- Kroto, H. W., Heath, J. R., O'Brien, S. C., Curl, R. F., & Smalley, R. E. 1985, *Nature*, 318, 162
- Kwok, S. 2009, *International Journal of Astrobiology*, 8, 161
- Leifer, S. D., Goodwin, D. G., Anderson, M. S., & Anderson, J. R. 1995, *Phys. Rev. B*, 51, 9973
- Micelotta, E. R., Jones, A. P., & Tielens, A. G. G. M. 2010a, *A&A*, 510, A36+
- 2010b, *A&A*, 510, A37+
- Nano-C. 2004, *Masters of the Flame: Industrial Production of Fullerenes Becomes a Reality* (<http://www.nano-c.com/technologies.as>)
- Pardo, J. R., Cernicharo, J., Goicoechea, J. R., Guélin, M., & Asensio Ramos, A. 2007, *ApJ*, 661, 250
- Peeters, E., Tielens, A. G. G. M., Allamandola, L. J., & Wolfire, M. G. 2012, *ApJ*, 747, 44
- Petrie, S., Stranger, R., & Duley, W. W. 2003, *ApJ*, 594, 869
- Rauls, E., & Hornekaer, L. 2008, *ApJ*, 679, 531
- Roberts, K. R. G., Smith, K. T., & Sarre, P. J. 2012, *MNRAS*, 421, 3277
- Rubin, R. H., Simpson, J. P., O'Dell, C. R., et al. 2011, *MNRAS*, 410, 1320
- Scott, A., & Duley, W. W. 1996, *ApJ*, 472, L123+
- Scott, A., Duley, W. W., & Pinho, G. P. 1997, *ApJ*, 489, L193+
- Sellgren, K., Werner, M. W., Ingalls, J. G., et al. 2010, *ApJ*, 722, L54
- Smith, F. W. 1984, *Journal of Applied Physics*, 55, 764
- Taylor, R., Hare, J. P., Abdul-Sada, A. K., & Kroto, H. W. 1990, *J. Chem. Soc., Chem. Commun.*, 1423
- Tielens, A. G. G. M. 2005, *The Physics and Chemistry of the Interstellar Medium* (Cambridge Univ. Press, Cambridge)
- Tomita, S., Andersen, J. U., Gottrup, C., Hvelplund, P., & Pedersen, U. V. 2001, *Phys. Rev. Lett.*, 87, 073401
- Ugarte, D. 1992, *Nature*, 359, 707
- Violi, A. 2004, *Combustion and Flame*, 139, 279
- Zhang, Y., & Kwok, S. 2011, *ApJ*, 730, 126
- Zheng, G., Irle, S., & Morokuma, K. 2005, *The Journal of Chemical Physics*, 122, 014708
- Zheng, G., Wang, Z., Irle, S., & Morokuma, K. 2007, *J. Nanosci. Nanotechnol.*, 7, 1662

## APPENDIX

### TIMESCALE FOR FULLERENE CONDENSATION IN SPACE

We report here the details of the calculation of the scaling rule (Eq. 1), which relates the time  $\tilde{\tau}$  required for fullerene condensation with the initial density  $n$  of the carbon gas. Consider an ensemble of  $N_p$  particles that can occupy  $N_v$  cells. The probability of having one particle in one cell is  $p = N_p/N_v \ll 1$ . The probability  $P$  of having two particles in the same cell at the same time is described by the Poisson statistics:

$$P(2; p) = \frac{p^2}{2} e^{-p} \quad (\text{A1})$$

We have that  $N_v \equiv V/\delta v$ , where  $V$  is the total volume and  $\delta v$  is the volume of a single cell. We can then rewrite the single occupancy probability as  $p = (N_p/V) \delta v = n \delta v$ .

The probability  $\tilde{P}$  of having interaction between two particles at time  $N_t$  can be written as:

$$\tilde{P}(\text{int}; N_t) = (1 - \lambda)^{N_t - 1} \lambda \quad (\text{A2})$$

where  $N_t \simeq t/\tau$ ,  $t$  being the time and  $\tau$  the characteristic time of a single interaction (depending on the nature of the interaction itself). The term  $\lambda$  represents the probability of interaction between two particles at a generic time  $t$ . The probability of having interaction between two particles up to the time  $N_t$  is then given by the following equation:

$$\tilde{P}(\text{int}; \leq N_t) = \sum_{k=0}^{N_t-1} (1 - \lambda)^k \lambda = 1 - (1 - \lambda)^{N_t} \quad (\text{A3})$$

If  $\lambda$  is small, we can rewrite Eq. A3 as:

$$\tilde{P}(\text{int}; \leq N_t) \simeq 1 - e^{-\lambda N_t} \simeq 1 - e^{-\lambda(t/\tau)} \quad (\text{A4})$$

The probability  $\lambda$  can be written in the following way:

$$\lambda = A P(2; p) \simeq A(n \delta v)^2 \quad (\text{A5})$$



The term  $A$  includes the characteristics intrinsic to the interaction (which we do not need to specify) while  $P(2; p)$  is the probability from Eq. A1. The approximation resulting in the right-hand term of the equation is valid for  $p \rightarrow 0$ . Combining Eqs. A4 and A5, with  $A\delta v^2 = B$ , we obtain

$$\tilde{P}(\text{int}; \leq N_t) \simeq 1 - e^{A(n\delta v)^2 (t/\tau)} \simeq 1 - e^{B n^2 t/\tau} \quad (\text{A6})$$

From Eq. A6 we can derive the timescale for condensation:

$$\tilde{\tau} = \frac{\tau}{n^2 B} \quad (\text{A7})$$

Because both  $\tau$  and  $B$  are independent from the initial particle density  $n$ , we can write the following scaling rule

$$\frac{\tilde{\tau}_2}{\tilde{\tau}_1} = \frac{n_1^2}{n_2^2} \Rightarrow \tilde{\tau}_2 = \frac{\tilde{\tau}_1 n_1^2}{n_2^2} \quad (\text{A8})$$

where  $\tilde{\tau}_1$  and  $\tilde{\tau}_2$  are the condensation timescales corresponding to densities  $n_1$  and  $n_2$  respectively.